International Journal of Advanced Technology in Engineering and Science
Vol. No.5, Issue No. 03, March 2017
www.ijates.com
ijates
ISSN 2348 - 7550

INFLUENCE OF SAMPLE'S THICKNESS ON Γ-RAY SHIELDING PARAMETERS

Kulwinder Singh Mann[1,2], Manmohan Singh Heer[3], Asha Rani[4]

[1]*Department of Applied Sciences, I. K. G. Punjab Technical University, Kapurthala, (India)*
[2]*Department of Physics, D.A.V. College, Bathinda-151001, Punjab, (India)*
[3]*Department of Physics, Kanya Maha Vidyalaya, Jalandhar-144001, (India)*
[4] *Department of Physics, Dev Samaj College for Women, Ferozpur-, Punjab, (India)*

ABSTRACT

Optimum-thickness (OT) value for low-Z materials has been estimated in measurement of total mass attenuation coefficient (μ_m, cm^2g^{-1}) for γ-rays using narrow-beam transmission geometry at three energies viz. 661.66, 1173.24, 1332.50 keV. OT is the maximum thickness (expressed in mean free path, mfp) of a sample used in μ_m measurements with good accuracy. The main objective of this study is to provide the missing information in the literature regarding OT value for low-Z materials. Six samples of commonly used low-Z building materials have been investigated. Monoenergetic γ-rays have been obtained from two standard radioactive sources (Cs^{137} and Co^{60}). The μ_m values have been measured using narrow-beam transmission geometry for particular sample at 13 different thickness values, starting from 2cm up to 26cm thus OT remains between 0.2-3.5mfp. A self designed and validated user friendly computer program, GRIC2-toolkit has been used for required theoretical computations. It has been concluded that for energy-range 661.66-1332.50 keV, the μ_m measurements of low-Z materials with γ-ray transmission-geometry, OT of 0.5mfp is considered as optimum-thickness value.

Keywords: Gamma-Ray Shielding Behaviour, Γ-Ray Shielding Parameters, Optimum-Thickness.

I INTRODUCTION

The experimental measurements of γ-ray shielding parameters (GSP) with good accuracy require perfect narrow-beam transmission-geometry. The total mass attenuation coefficient (μ_m, cm^2g^{-1}) is the most important GSP, because many other GSP can be derived from it. μ_m is useful in applications such as non-destructive analysis (NDA) of materials and CT-scan [1]. Thus, high accuracy of μ_m measurement is essential. However, practical γ-ray transmission-geometry used for μ_m measurements usually deviates from the perfect-narrowness. This deviation may be due to intermixing of scattered photons while traversing the γ-ray beam through a material, causing error in measured values of μ_m. Variations of the μ_m values with absorber (sample) thickness have been pointed in the literature [2-5]. In such variations, Varier et al., have reported the opposite trend than others. But, they have not explained the cause of this type of trend. Other researchers have concluded that for accurate measurements of μ_m, the sample's thickness may be up to 1mfp [2-4]. However, these results are

restricted to high-Z materials, e.g. Fe, Cu, Hg, Pb, etc. The maximum thickness (expressed in mean free path, mfp) of the sample placed in the narrow-beam transmission-geometry, under which it can be used for μ_m measurement is termed as optimum-thickness. Thus, in other words, sample's thickness up to its optimum-thickness can be used for μ_m measurements with good accuracy. Thus, for high-Z materials, the optical thickness of 1mfp has termed as optimum-thickness. To the best of our knowledge the information regarding the optimum-thickness for low-Z materials was missing in the literature.

In this study the optimum-thickness values for some low-Z materials have been estimated using μ_m measurements with γ-ray transmission narrow-beam geometry [6] at three energies viz. 661.66, 1173.24, 1332.50keV.

The μ_m is the most important GSP as values of parameters such as HVL, TVL, effective atomic-number (Z_{eff}), effective electron density ($N_{el,eff}$), effective atomic-weight (A_{eff}), and BUF depend on it. For a material, the accuracy in GSP is useful to know its γ-ray shielding behaviour (GSB).

II OBJECTIVE

The main objective of this study is to provide the missing information in the available literature regarding the optimum-thickness value for low-Z materials.

III THEORY

The ANS-standards [7] have defined the 'mean free path' (mfp) as the average distance that a monoenergetic photon travels between consecutive interactions in a given material. Mathematically, it is equal to the reciprocal of the linear attenuation coefficient, μ of the material. As per the Lambert-Beer's law [8-10]:

$$I = I_0 e^{-\mu t} \tag{1}$$

Where, I_0 represents the incident intensity of the beam (without the slab), I represents the transmitted intensity (in the presence of slab of material with thickness t expressed in cm) and μ is termed as total linear attenuation coefficient (cm^{-1}) of the material for γ-ray. Thus, probability that a photon can travel distance t without any interaction is given by $\exp(-\mu t)$, Eq. (1). Thus, the mean free path (mfp) can be calculated as:

$$\text{mfp} = \frac{\int_0^\infty t e^{-\mu t} dt}{\int_0^\infty e^{-\mu t} dt} = \frac{1}{\mu} \tag{2}$$

Hubbell [11] has defined mass attenuation coefficient as:

$$\mu_m = \mu/\rho = x^{-1} \ln\left[I_o / I(x)\right] \tag{3}$$

where, $I(x)$ represents the intensity of the transmitted ray noted with the thin material-slab placed in its path, x represents the mass thickness (mass per unit area, g cm^{-2}) of the material-slab.

The sample-thickness t (along the beam) in ordinary units (cm) can be converted into dimensionless-thickness, the OT, ($X=\mu.t$) expressing the thickness as the number of mfp lengths [7]. Thus, for an absorber (sample) with OT of 1mfp, its physical (linear) thickness can be obtained as: $t=1/\mu$. For a monoenergetic γ-ray, it has been

found that the μ value of a low-*Z* material is always smaller that its value for any high-Z material [12-15]. Thus, for the fixed energy and the OT of 1mfp, the linear thickness (*t*) of low-Z material is comparatively large as compared to any high-Z material. The ANS-standards suggest that the number of scattered photons increases with the increase in material's thickness. Thus, for samples of similar OT thickness values, the scattered photons contribute more for low-Z material than high-Z material. ANS-standards also support this observation by showing a decreasing trend in BUF values, with increase in atomic-number (Z).

IV MATERIALS AND METHODS

4.1 Materials

The investigation has been completed with six samples of easily accessible low-Z building materials. The easy availability and reproducibility of the selected samples as per Indian standards [16-20] are the reasons behind their selection. The chemical compositions of samples have been measured with WDXRF-technique (BRUKER, model S8-TIGER) at SAIF/CIL (Sophisticated Analytical Instrumentation Facility and Central Instrumentation Laboratory), Panjab University, Chandigarh. Fundamental details, measured values of chemical compositions of, measured values of linear thickness (along the beam) and corresponding computed OT for the of the selected samples have been provided in our previous publication [1].

Three monoenergetic γ-rays were obtained from the point-isotropic radioactive sources, Cs^{137} (100mCi) and Co^{60} (10mCi) procured from Board of Radiation and Isotope Technology (BRIT), Bhabha Atomic Research Centre (BARC), Trombay, Mumbai, India. The handling and storing of these strong sources were performed as per ICRP and AERB recommendations. Gamma-ray intensities were measured and recorded with NaI(Tl) scintillation detector (Canberra, model: 802) coupled with MCA (2k channels, plug-in-card, ORTEC) and MAESTRO computer software. The complete detector assembly was kept at suitable distances from all sides of the laboratory viz. walls, floor, and ceiling. To protect the detector assembly from the background and other radiations (fluorescent and scattered), the complete experimental setup was shielded with lead-alloy blocks (of thickness≈8cm). The lead-alloy blocks used to construct the first layer of the shield towards the beam, were wrapped in Aluminium sheet (of thickness≈1.15mm) to minimize the chances of bremsstrahlung radiations. The experimental measurements were performed in the Radiation Laboratory of SLIET, Longowal. A narrow-beam transmission geometrical setup has been adopted for the measurements using NaI(Tl) detector assembly.The stability and reproducibility of experimental setup were verified using a reference absorber (Aluminium sheet, procured from Sigma-Aldrich) at 661.66keV. To avoid any shift in the photo-peak during the experiment, various physical parameters of the laboratory were controlled by continuously running air conditioners. To minimize the statistical error (<1%) the real-time of the detector was taken as 1200s for each measurement [21].

Theoretical computations have been performed using the self-designed computer program, GRIC2-toolkit [1]. GRIC2-toolkit is the modified form of GRIC-toolkit [22] with extended capabilities. Both experimental and theoretical results have been compared to verify the influence of the sample's thickness on the measured values of μ_m thereby ascertain the optimum-thickness value for the low-Z materials.

This investigation has been preformed for 13 thickness values of each sample, using the same experimental setup. This was necessary to verify the influence of optimum-thickness value on GSP for low-Z materials.

4.2. Methodology

4.2.1. Experimental details

The narrow-beam transmission-geometry and test of geometry for narrowness [6] have been provided in our previous work [1].

Table 1. The measured and computed values of densities, mass attenuation coefficients and uncertainties at three energies, for two thickness values of samples (Mann et al., 2015b).

Sample	Density ($g\ cm^{-3}$)	Thickness (cm)	Mass attenuation coefficients (μ_m) cm^2g^{-1}					
			^{137}Cs (661.66 keV)		^{60}Co (1173.24 keV)		^{60}Co (1332.50 keV)	
			Experimental	Theo.	Experimental	Theo.	Experimental	Theo.
CB	1.652	3.35	0.0773 ±0.0024	0.0774	0.0598 ±0.0028	0.0586	0.0557 ±0.0016	0.0549
CB'	1.652	9.26	0.0792 ±0.0027	0.0774	0.0579 ±0.0028	0.0586	0.0566 ±0.0016	0.0549
CW	1.826	3.05	0.0793 ±0.0024	0.0777	0.0602 ±0.0029	0.0588	0.0562 ±0.0016	0.0551
CW'	1.826	9.28	0.0804 ±0.0028	0.0777	0.0613 ±0.0029	0.0588	0.0599 ±0.0017	0.0551
CY	1.743	4.59	0.0751 ±0.0023	0.0768	0.0571 ±0.0027	0.0583	0.0534 ±0.0015	0.0547
CY'	1.743	8.67	0.0790 ±0.0027	0.0768	0.0609 ±0.0029	0.0583	0.0622 ±0.0018	0.0547
RM	1.855	3.94	0.0770 ±0.0024	0.0769	0.0582 ±0.0028	0.0584	0.0533 ±0.0015	0.0547
RM'	1.855	9.16	0.0760 ±0.0026	0.0769	0.0572 ±0.0027	0.0584	0.0574 ±0.0017	0.0547
LS	1.072	3.21	0.0788 ±0.0024	0.0780	0.0592 ±0.0028	0.0589	0.0555 ±0.0016	0.0552
LS'	1.072	9.18	0.0794 ±0.0027	0.0780	0.0599 ±0.0029	0.0589	0.0596 ±0.0017	0.0552
PP	1.253	3.13	0.0773 ±0.0024	0.0776	0.0583 ±0.0028	0.0588	0.0549 ±0.0016	0.0551
PP'	1.253	9.43	0.0807 ±0.0028	0.0776	0.0617 ±0.0029	0.0588	0.0622 ±0.0018	0.0551

Table 2. Detail of computed values of additional GSP of the selected materials

Energy	CB		CW		CY		RM		LS		PP	
(keV)	Exp.	Theo.	Exp.	Theo.	Exp.	Theo.	Exp.	Theo.	Exp.	Theo.	Exp.	Theo.
						Effective atomic-weight (A_{eff})						
661.66	23.628	23.867	24.081	24.826	21.396	21.612	21.323	21.538	27.399	27.676	22.369	22.826
1173.24	23.619	23.858	24.322	24.818	21.390	21.606	21.317	21.532	26.836	27.666	22.135	22.820
1332.5	23.146	23.862	24.574	24.822	21.177	21.609	21.104	21.535	26.841	27.671	22.596	22.824
						Effective atomic-number (Z_{eff})						
661.66	11.535	11.892	12.289	12.413	10.455	10.778	10.419	10.741	13.565	13.842	11.211	11.440
1173.24	11.530	11.887	12.160	12.408	10.559	10.774	10.416	10.738	13.421	13.836	11.322	11.436
1332.5	11.649	11.887	12.284	12.408	10.559	10.774	10.523	10.738	13.559	13.836	11.322	11.436
						Total interaction cross-section, σ_{tot} (barn)						
661.66	3.042	3.048	3.175	3.178	2.746	2.754	2.740	2.745	3.543	3.547	2.915	2.924
1173.24	2.315	2.320	2.412	2.419	2.095	2.097	2.087	2.091	2.697	2.700	2.223	2.227
1332.5	2.174	2.176	2.263	2.268	1.965	1.967	1.954	1.960	2.524	2.532	2.082	2.088
						Effective electron density, $N_{el,eff}$ ($\times 10^{23}$ electrons g^{-1})						
661.66	2.984	2.987	3.001	3.004	2.971	2.974	2.969	2.975	2.998	3.007	2.998	3.007
1173.24	2.980	2.986	2.994	3.003	2.970	2.973	2.968	2.974	2.997	3.006	2.998	3.007
1332.5	2.977	2.986	2.994	3.003	2.965	2.974	2.966	2.975	3.004	3.007	3.004	3.007

4.2.2 Measurements

Gamma-ray's photo-peak intensities without any sample (I_o) and with the sample (I) placed between the source and the detector were measured and corrected for background counts. The background counts were noted for the same real-time without placing the source in geometry. The counting-rates (counts/s) for each sample-brick were obtained by dividing the recorded counts by the live-time of the detector. Thus, at selected energy, the μ_m values of each sample were computed by putting the recorded data in Eq. (3). The measurements for each sample and energy were repeated for at least four times. The arithmetic-mean of the computed values of μ_m has considered as the experimental value. For fixed energy, variations in μ_m value in the sample-brick thickness, was studied in two steps. Step1: the measurements were made at two orientations of the same sample-brick (placing the sample along the beam, first lengthwise and then breadth wise). The comparison of all such measured and computed values has been shown in Fig. 1. The noted values of γ-ray photo-peak-counts were normalized to the

same energy. In above measurements, slight variations in μ_m values with sample-thickness were noticed. Step2: the measurements were repeated for each sample by varying its thickness in rage (2-26 cm) using the same experimental setup. For three γ-ray energies and each selected sample, the measured values of μ_m were compared with their theoretical values (GRIC2-toolkit) to establish the optimum-thickness value.

The physical parameters such as mass, dimensions and density of the sample-bricks were measured using an electronic balance of accuracy ±0.01g, and the digital vernier calipers of accuracy ±0.02mm. The densities of the sample-bricks were obtained by the standard method [23].

4.2.3. Calculations

The theoretical values of μ_m for the samples were computed from their chemical compositions with the aid of self-designed GRIC2-toolkit [1]. The measured and computed values of μ_m have been listed in Table 1. The measured and computed values of some additional GSP viz. effective atomic number (Z_{eff}), effective atomic weight (A_{eff}), effective electron density ($N_{el,eff}$) and total interaction coefficients (σ_{tot}) have been provided in the Table 2. Keeping in view the optimum-thickness, the measured values of μ_m for the samples were considered as their experimental values.

V RESULTS AND DISCUSSION

5.4.1 Errors

The total error in the measured value of μ_m depends on the corresponding errors of incident intensity (I_o), transmitted intensity through the sample (I), thickness of the sample (t) and its density (ρ). The errors in the measured values have been computed by Eq. (4) [24].

$$\Delta\mu_m = \frac{1}{\rho.t}\sqrt{\left(\frac{\Delta I_o}{I_0}\right)^2 + \left(\frac{\Delta I}{I}\right)^2 + \left(\ln\frac{I_o}{I}\right)^2 \times \left[\left(\frac{\Delta\rho}{\rho}\right)^2 + \left(\frac{\Delta t}{t}\right)^2\right]} \quad (4)$$

Where ΔI_o, ΔI, $\Delta\rho$ and Δt are errors in corresponding quantities. These errors were mainly due to fluctuations in counting statistics of photo-peak counts, dead time of the detector and deviation of the geometry from the perfect-narrowness. The respective errors have been listed in Table 1.

5.4.2 Optimum-Thickness

Fig. 1 indicates that for two thickness values of each sample listed in Table 1, the measured values of μ_m at three γ-ray energies almost agreed with their theoretical values with minor deviations. These deviations may be either due to statistical errors in the measured values of μ_m or due to the intermixing of scattered photons with transmitted γ-ray beam. In order to find the actual reason for such deviations, following approach has been adopted:

International Journal of Advanced Technology in Engineering and Science
Vol. No.5, Issue No. 03, March 2017
www.ijates.com
ijates
ISSN 2348 - 7550

5.4.2.1 Validate chemical composition.

Fig. 2 shows a very good agreement between the computed values of μ_m, from sample's chemical compositions obtained with two techniques i.e. WDXRF and XRD-R`. Thus, the chemical compositions of the sample have been cross-checked for the accuracy of theoretical computations.

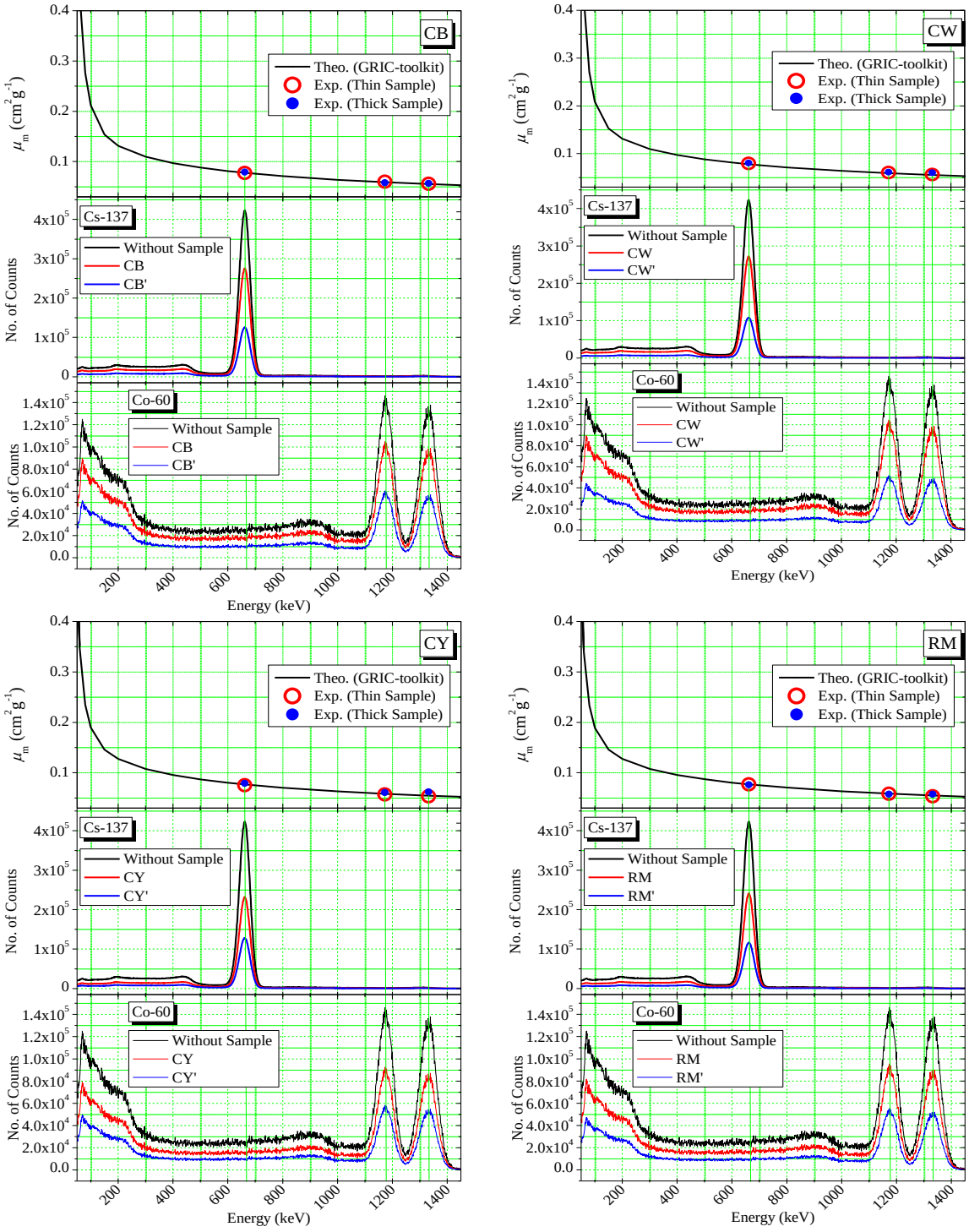

International Journal of Advanced Technology in Engineering and Science
Vol. No.5, Issue No. 03, March 2017
www.ijates.com
ijates
ISSN 2348 - 7550

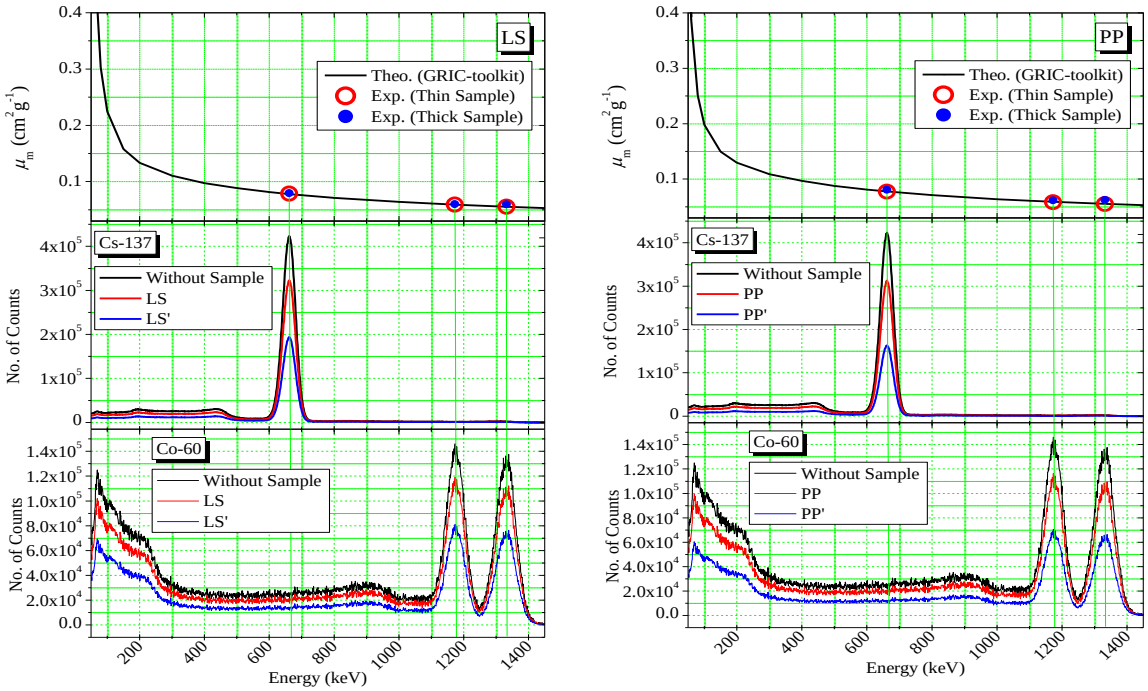

Figure 1 Comparison of theoretical and experimental values of mass attenuation coefficients for three γ-ray energies and transmission γ-ray spectra (after subtracting background counts) through the selected samples (CB, CW, CY, RM, LS and PP) for two thickness values of each sample.

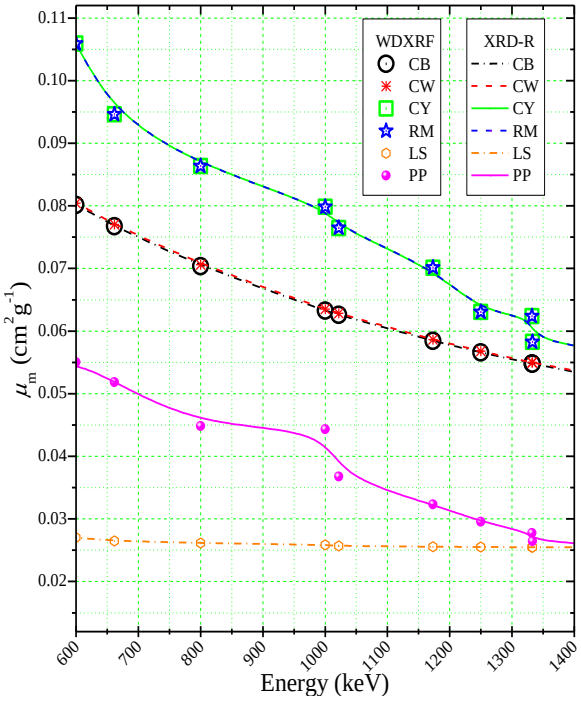

Figure 2 Similarity of GRIC2-toolkit computed values of mass attenuation coefficients for sample's compositions obtained by two techniques (WDXRF and XRD-R).

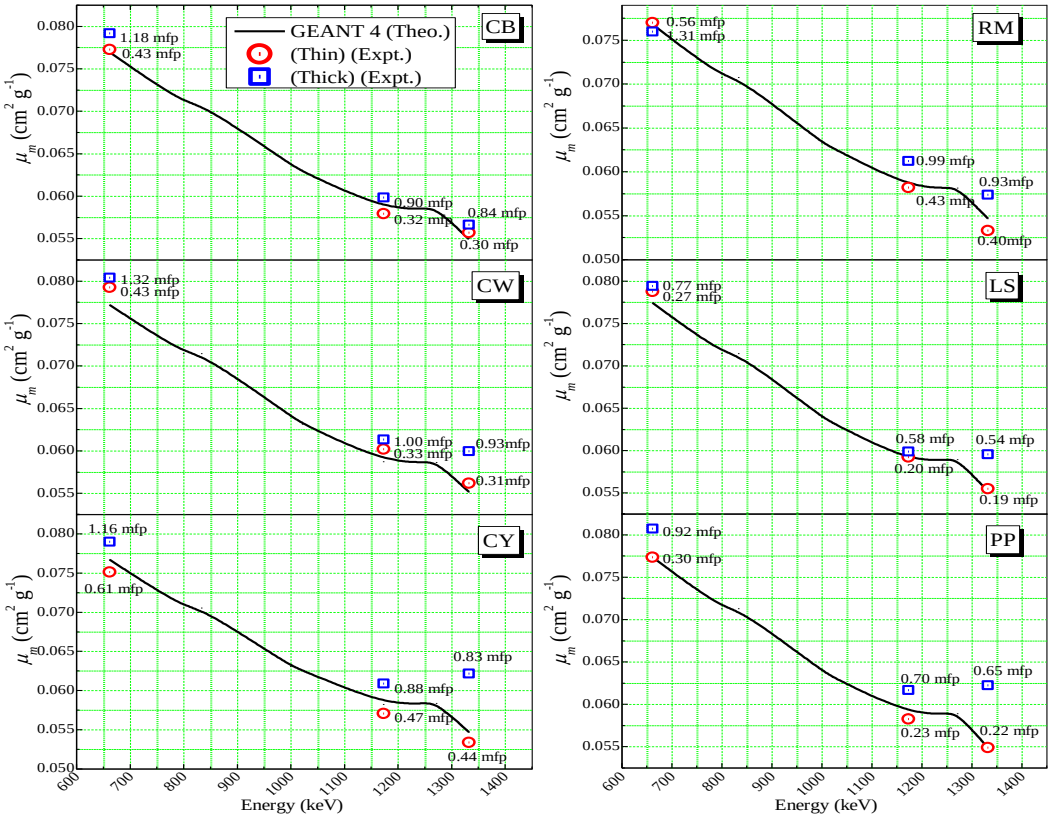

Figure 3 Comparison of experimentally measured and Monte Carlo simulated values of μ_m for the chosen samples, at three energies.

5.4.2.2 Contradiction.

Table 1 indicates that the measured values of μ_m agreed fairly well with the corresponding theoretical values for thin samples with OT≤0.5mfp. However, for comparatively thick samples with OT>0.5mfp, the agreement was not good. This finding has been reconfirmed by using the Monte Carlo simulation toolkit (GEANT4). Fig. 3 shows the measured and computed values (GEANT4-toolkit) of μ_m for both thin (OT≤ 0.5mfp) and thick (OT>0.5mfp) samples. Both toolkits (GRIC2 and GEANT4) have indicated the similar results.

Varier et al., [5] have confirmed similar variations in the experimental value of μ_m with the sample's thickness. According to them the experimental values μ_m decreases with the increasing sample's thickness above 1mfp (1<OT<5.5mfp). However, they have not explained the cause of this trend. In contradiction, various researchers [2-4] have reported the opposite trend that the measured values of μ_m increases with the increase in the sample's thickness, and the true value of μ_m was suggested to obtain by extrapolation of the sample-thickness to zero. Thus, they have suggested that the sample's thickness should remain below 1mfp to improve the accuracy in μ_m measurements. However, they also have not provided the explanation and cause of such observations.

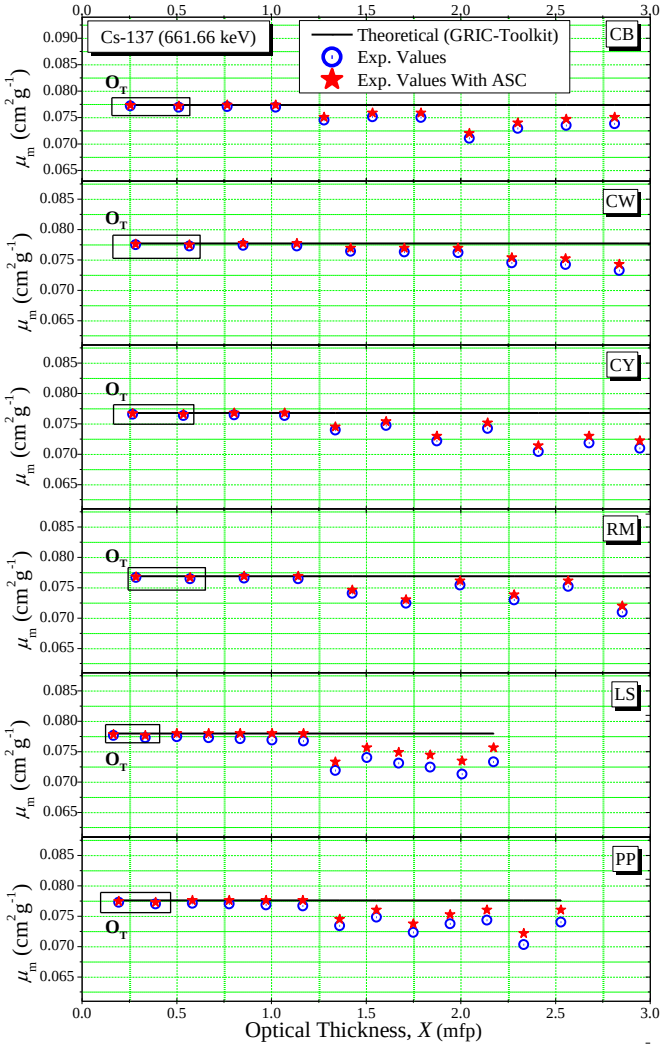

Figure 4 Comparison of the experimentally measured and computed values of mass attenuation coefficients of the samples for Cs^{137}.

5.4.2.3 Measurements at more thickness values.

To check the influence of the sample's thickness on its measured μ_m values, the sample-brick thickness was varied from 2-26cm ($0.2 \leq OT \leq 3.5$mfp), in steps of 2cm using 13 similar bricks of each sample. The similar procedure has been adopted for the preparation of new bricks as adopted previously. Other parameters such as density and transverse dimensions (breadth and height) of these bricks were in conformity with the previously used bricks. The same narrow-beam geometrical setup [1] has been used for measurements. The average of four measurements has been considered as the experimental value of μ_m. Figs. 4 and 5 have shown the theoretically computed and experimentally measured values of μ_m at various OT values for all samples at three energies of γ-rays. The observed trend of μ_m variations with the OT is in agreement with that suggested by Varier et al., [5] but in our case the lower limit of the OT has been modified to 0.5mfp from 1.0mfp. So it has been concluded that for low-Z materials, the 0.5mfp OT is the optimum value of the sample's thickness for its μ_m measurement

with good accuracy. Thus, 0.5mfp OT is termed as the optimum-thickness for low-Z materials in the selected energy-range (661.66-1332.50keV).

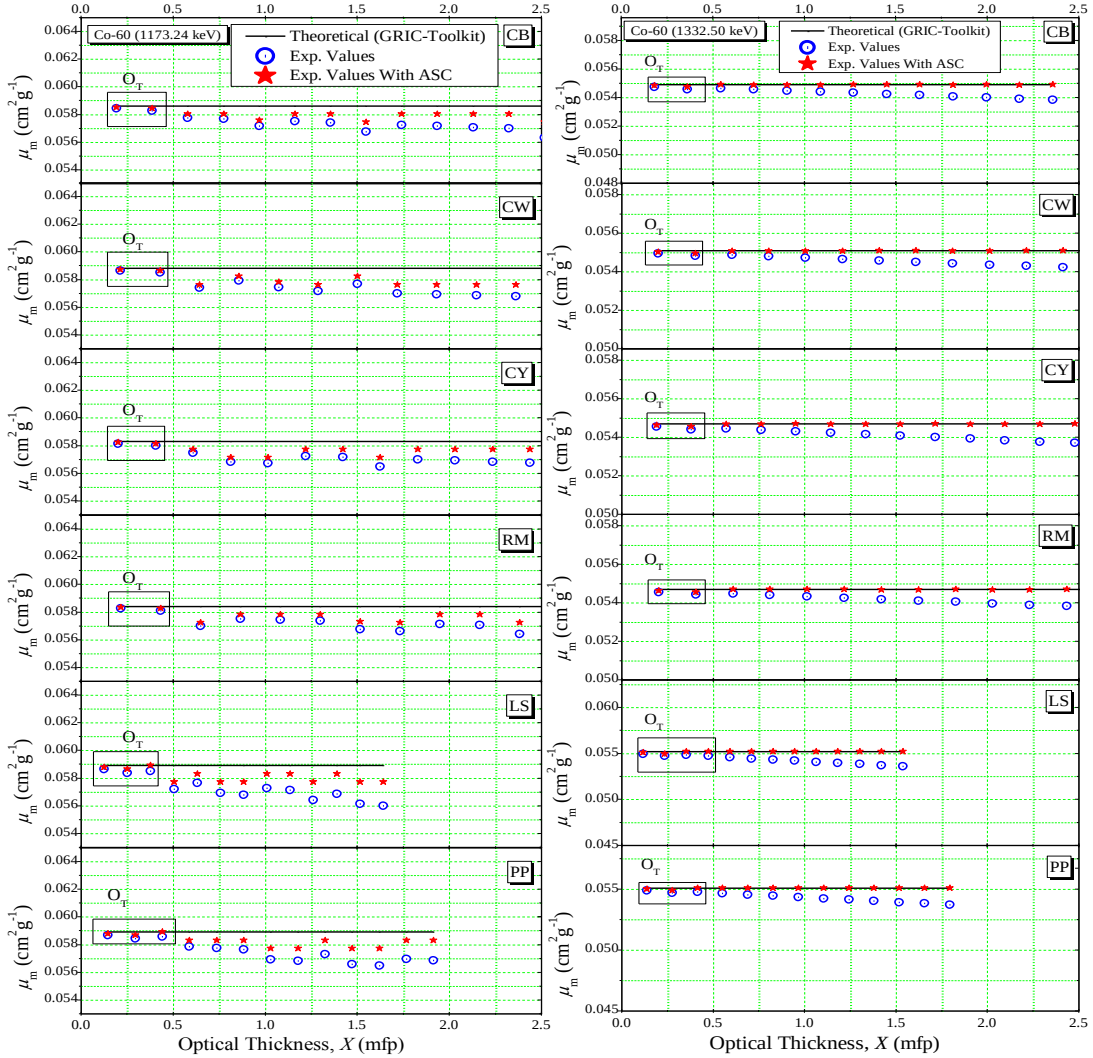

Figure5 Comparison of the experimentally measured and computed values of mass attenuation coefficients of the samples for Co^{60}.

5.4.2.4 Explanation of findings with mathematical model.

The positive relationship between the measured value of μ_m and sample's thickness has been attributed to the influence of the Compton-scattered-radiations. A mathematical model has been suggested to explain the cause of the present observations as follows:

Though, narrow-beam geometry was established for present measurements, but perfect narrow-beam geometry can never be achieved practically. Thus, the chances of scattered-radiations are always there to enter in the detector along with the transmitted beam, which accounts for BUF, *B.* In such a case, the intensity of the transmitted beam can be explained by the modified Lambert-Beer's law [25]:

$$I=B.I_o.e^{-\mu.t}.$$

$$\Rightarrow \mu = \frac{\ln(I_o/I)}{t} + \frac{\ln(B)}{t} \qquad \Rightarrow \mu = \mu_{\text{exp.}} + \frac{\ln(B)}{t}$$

$$\therefore \quad \mu_{\text{exp.}} = \mu - \frac{\ln(B)}{t} \tag{5}$$

Where, μ represents the theoretical linear attenuation coefficient and t represents thickness of sample-brick along the beam. Since, I represents experimental transmitted intensity, the term, $\ln(I_o/I)/t$, gives the experimental value of the linear attenuation coefficient, μ_{exp}.

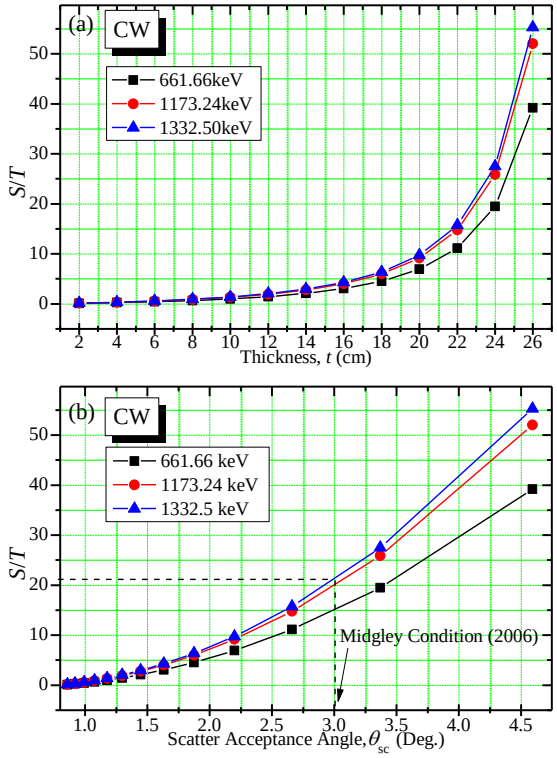

Figure 6 Variation of scattered to transmitted ratio with sample-thickness, at the three energies.

For practical narrow-beam geometry, ratio of scattered to transmitted (S/T) photons entering into the detector has been evaluated by the analytical-formula [26]: $S/T = N_{\text{el,eff}}.t.\sigma_{\text{c},\theta\text{sc}}$. Where, $N_{\text{el,eff}}$ represents the effective electron density of the sample, $\sigma_{\text{c},\theta\text{sc}}=\Pi r_o^2{}_{\theta\text{sc}}{}^2$ gives the Compton interaction cross-section of the photons, scattered for the θ_{sc} (scatter acceptance angle), and r_o represents the electron radius, 2.818×10^{-15}m. Fig. 6 shows that with increase in sample's thickness, t the value of S/T increases as a result B value also increases thereby μ_{exp} value decreases (Eq. 5). Thus, it has concluded that with the increase in sample's thickness, the measured value of μ_{m} goes on decreasing. Thereby it has been confirmed that variation in the measured value of μ_{m} is due to the intermixing of scattered photons with the transmitted beam.

VI CONCLUSIONS

It has been concluded that for the measurements of GSP using γ-ray transmission-geometry, for low-Z materials in energy-range 661.66-1332.50keV, the optical-thickness (OT) of 0.5mfp is considered as the optimum-thickness value.

The deviations between measured and theoretical values of μ_m have been caused due to the influence of scattered photons and statistical errors. The contributions of these factors go on increasing with thickness of the sample, results in further deviation in μ_m.

ACKNOWLEDGEMENTS

Authors are grateful to SAIF/CIL, Punjab University, Chandigarh for accurately estimating chemical compositions of the selected samples using WD-XRF-facility. The present work is devoted to the Ph.D-thesis under Pre.Reg.Number:1311025, Punjab Technical University, Kapurthala.

REFERENCES

[1] K.S. Mann, M.S. Heer, A. Rani, Effect of low-*Z* absorber′s thickness on gamma-ray shielding parameters, Nucl. Instrum. Methods A, 797, 2015, 19-28.

[2] S. Gopal, B. Sanjeevaiah, A method to determine the γ- ray attenuation coefficients, Nucl. Instr. and Meth., 107, 1973, 221-225.

[3] G.S. Sidhu, P.S. Singh, G.S. Mudahar, Energy absorption buildup factor studies in biological samples, Radiat. Prot. Dosim., 86, 1999, 207-216.

[4] M. Singh, G. Singh, B.S. Sandhu, B. Singh, Effect of detector collimator and sample-thickness on 0.662 MeV multiply Compton-scattered gamma-rays, Appl. Radiat. Isot., 64, 2006, 373-378.

[5] K.M.Varier, S.N. Kunju, K. Madhusudhanan, Effect of finite absorber dimensions on γ-ray attenuation measurements, Phys. Rev. A, 33, 1986, 2378-2381.

[6] S. Midgley, Angular width of a narrow-beam for X-ray linear attenuation Coefficient Measurements, Radiat. Phys. Chem., 75 (9), 2006, 945-953.

[7] ANSI/ANS 6.4.3-1991 (W2001), Gamma-ray attenuation coefficients and buildup factors for engineering materials, American Nuclear Society, La Grange Park, Illinois.

[8] P. Bouguer, Essai d'Optique sur la Gradation de la Lumi`ere (France: Havre, 1729).

[9] A. Beer, Bestimmung der Absorption des roten Lichts in farbingen Fl¨ussigkeiten," Ann. Phys., Lpz., 86, 1852, 78–88.

[10] J. H. Lambert, Photometria sive de Mensura et Gradibus Luminis Colorum et Umbrae Augsburg, Germany, 1760.

[11] J. H. Hubbell, Experimentally measured total X-ray attenuation coefficients extracted from previously unprocessed documents held by the NIST Photon and Charged Particle Data Center, II NISTIR, 2004, 7163.

[12] M. J. Berger, J. H. Hubbell, XCOM: Photon cross- sections database, Web version1.2, Natl. Ins. Standards Tech., Gaithersburg, MD 20899, originally published as NBSIR, 87, 1987, 3597.

[13] J. H. Hubbell, S.M. Seltzer, Tables of X-raymass attenuation coefficients and mass energy absorption coefficients 1 keV to 20 MeV for elements Z = 1 to 92 and 48 additional substances of dosimetric interest, NISTIR, 1995, 5632.

[14] D. E. Cullen, J. H. Hubbell, L. Kissel, EPDL97: the evaluated photon data library Lawrence Livermore National Laboratory Report, UCRL-50400, 1997.

[15] M.B. Chadwick, P. Oblozinsky, M. Herman et al., ENDF/B-VII.0: Next generation evaluated nuclear data library for nuclear science and technology, Nucl. Data Sheets 107, 2006, 2931–3060.

[16] IS: 1128 (1974), Specification for limestone (slab and tiles) (first revision), Bureau of Indian Standards, New Delhi, India. [Reaffirmed in 2013].

[17] IS: 2720-part 40, (1977), Indian Standard Methods of Testing for Soils: Determination of Free Swell Index of Soils, BIS, New Delhi.

[18] IS: 2542-part1-12 (1978), Methods of Test for Gypsum Plaster, Concrete and Products, Part I: Plaster and Concrete, Bureau of Indian Standards, New Delhi, India.

[19] IS: 8042 (1989), Specification for white Portland cement (second revision), Bureau of Indian Standards, New Delhi, India. [Reaffirmed in 2014].

[20] IS: 3812-part1 (2013), Specification for Pulverized Fuel Ash, Part 1: For Use as Pozzolana in Cement, Cement Mortar and Concrete, 3rd revision, Bureau of Indian Standards, New Delhi, India.

[21] G. Dale, Simply Managing Dead Time Errors in Gamma-Ray Spectrometry, Application Note AN63, http://www.ortec-online.com/

[22] K.S. Mann, A. Rani, M.S. Heer, Shielding behaviours of some polymer and plastic materials for gamma-rays, Radiat. Phys. Chem., 106, 2015, 247-254.

[23] ASTM D 854, (2014), Standard Test Methods for Specific Gravity of Soil Solids by Water Pycnometer, ASTM International, West Conshohocken, PA.

[24] N. Celik, U. Cevik, A. Celik, Effect of detector collimation on the measured mass attenuation coefficients of some elements for 59.5–661.6 keV gamma-rays, Nucl. Instr. Meth. B, 281, 2012, 8-14.

[25] S.P. Singh, T. Singh, P. Kaur, Variation of energy absorption buildup factors with incident photon energy and penetration depth for some commonly used solvents, Ann. Nucl. Energy, 35, 2008, 1093–1097.

[26] C. M. Davisson, R. D. Evans, Gamma-Ray absorption coefficients, Rev. Mod. Phys., 24, 1952, 79-107.